

CONTROL SYSTEM DESIGN FOR MULTI-ROTOR MAV

WEI WANG, HAO MA

College of Information and Control, Nanjing University of Information Science and Technology, Nanjing, China

CHANG-YIN SUN

School of Automation, Southeast University, Nanjing, China

w-mail: wucb@nuist.edu.cn

Abstract MAVs (Micro Air Vehicles) have attracted more and more attention in recent years because of their wide applications, such as investigations of inhospitable environment, nuclear or hazardous material polluted regions and other inaccessible areas. In this paper, both attitude and altitude controls of a Quad-Rotor type MAV are discussed and analyzed. To stabilize the attitude, one order memory based controller is selected, the performance of which is independent of the detail model information, leading to enhanced robustness. While for the altitude, a Linear Quadratic Gaussian (LQG) controller is proposed. The experimental results of the real flight demonstrate the stability and robustness of the controllers.

Key words: MAV, attitude control, altitude control, LQG, memory based control

1. Introduction

Recently, a new class of flight vehicles, called Micro Air Vehicles (MAVs) which have great potential for military, industrial as well as civilian applications, has gained tremendous attention. Since the 1990s, with the development of the Micro Electro Mechanical System (MEMS) technology, a single rotor helicopter has been the favorable platform for MAV development. However, the disadvantages such as complexity, instability and limited payload slowed down its development. While the multi-rotor vehicle, especially the Quad-Rotor vehicle, is studied in more research experiments. The Quad-Rotor MAV, compared with a single rotor helicopter and dual-rotor vehicle, has excellent capabilities of small size, superior payload, low cost and simple manufacture. As a result, it can be widely used in military reconnaissance, meteorological survey, environmental monitoring and air transportation in emergency and other aspects (Martinez, 2007).

Normally, MAVs need to fly autonomously to accomplish those difficult missions. However, many technical difficulties are induced by their small sizes and structures, especially the installation of communication apparatus and sensors. Until now, tremendous achievements have been made in solving these difficulties by many groups and institutions such as MIT, Ascending Technology, Microdrones, Draganfly, Heudiasyc University, Pennsylvania University and Chiba University (Achtelik et al, 2009; Bachrach et al, 2009; [2], [5], Wanget al, 2008; Nonami et al, 2010). To realize an autonomous flight, various types of control techniques have been proposed, including back stepping (BS), nonlinear control, robust control and so on (Kendoul, 2012, Tayebi and McGilcary, 2006; Xia et al, 2012). Recently, the discussion of flight control has been driven to a mature stage and the focus of MAV research has been transferred to the vision based flight, indoor obstacle avoidance (Hoffman et al, 2011), SLAM based control (Rudin et al, 2011) or the development of new structure MAVs. Despite that, the performance of all flight controllers is limited by the external disturbance and model errors. Therefore, only in certain circumstances can they well operate. Maybe it is not serious for research study, but when it is used for practical

application, the environmental restriction will be a remarkable imperfection. So it is still of great significance to develop a really effective robust controller.

In this paper, the main considerations of system dynamics of attitude and altitude motions as well as the control algorithms are discussed. With the control input and output of the real plant obtained by flight experiments, the mathematical model can be obtained by system identification tools in Matlab. To achieve the attitude control, we apply a memory based controller which makes use of certain historical information to build the control scheme. The greatest attractiveness of this algorithm is that the control performance is not related to the detail of system dynamics and outer disturbances, so that significant robustness is maintained. As to the altitude, we use a barometer and accelerometer instead of the widely used GPS to improve the precision. Then a model based optimal controller is applied. A Kalman filter is also applied to filter the noise and estimate the unobserved state variables.

2. Controlled object

Our research platform is a 4-channel radio controlled Quad-Rotor MAV designed by our research group. The vehicle has a carbon fiber airframe, which provides great stiffness and rigidity while keeps the weight down. The lift results from four AKE brushless motors. In order to drive these brushless motors, Pentium-18A Ultra-PWM brushless driver which can support 50 Hz-500 Hz PWM signal communication is selected. With the brushless driver, the maximum speed can reach about 8000 rpm and payload of about 1 kg can be acquired at the same time with four propellers of APC1245. The flight time is about 10 minutes with a three-cell-2100mAh LiPo battery without payload. Figure 1 shows an overview of our platform. And the specification is shown in Table 1.



Fig. 1. Quad-Rotor type MAV

Table 1. Specification of Quad-Rotor type MAV

Parameter	Value	Unit
Maximum diameter	500	mm
Height	250	mm
Total mass	1.1	kg
Maximum lift	1.0	kg

The embedded control system consists of one IMU sensor XSENS, one triaxial accelerometer, one barometer, one 12 bit ADC chip MCP3204 and one Arm7 micro controller. The navigation

data for attitude control are read from the XSENS through an RS-232 serial communication. To improve the accuracy of altitude information, a triaxial accelerometer ADXL335 from Analog Devices Corporation together with an MPX5100Ap barometer is supplied to the Kalman filter for estimation. The Arm7 receives control instruction by a 72 MHz PPM receiver and sensor data to run independent control loops for each axis. The entire processing is done with a control loop frequency of 400 Hz. The configuration of the overall system can be seen in Fig. 2. In order to obtain the flight data and prepare for the future research, communication between the vehicle and the ground control station is accomplished at the frequency of 50 Hz via a wireless modem XBee-pro which can communicate up to 1.6 km with its maximum power of 63 mW.

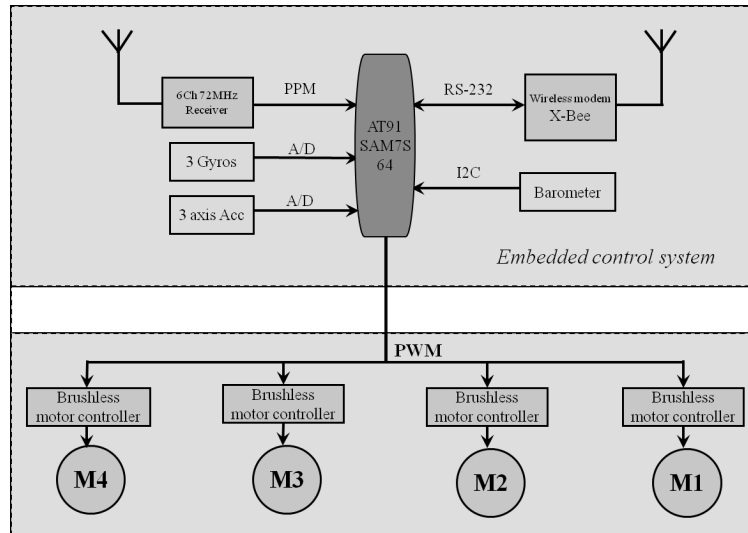


Fig. 2. Configuration of Quad-Rotor system

3. Attitude modeling and controller design

This section mainly illustrates the attitude modeling and controller design. Generally, for the X and Y directions, we divide the autonomous flight control loop into three loops: attitude, velocity, and position. Therefore, the first step is to accomplish the attitude control, which directly affects the flight performance.

In view of the inevitable nonlinearity and the uncertain outer disturbances, it is impossible to generate the accurate attitude model. Therefore, it is of great importance to design a controller with strong robustness. In this section, a one order memory based controller is recommended. The fundamental idea of the control algorithm is to utilize certain memorized information such as the current system response, previous system response and past control experience to build control action. The main advantage of this approach is that the controller performance has no relation to the detail of system dynamics. In addition, the overall required memory space does not grow with time and is much smaller than most existing learning control methods.

3.1. Attitude modeling

Tuning of rotational speed of every rotor leads to every degree of freedom of the Quad-Rotor, therefore, the coupled motion is very obvious. However, it is quite difficult to analyze such a multiple-input and multiple-output (MIMO) system. For simplification, the modeling of the nonlinear attitude motion is carried out on the premise of neglecting the coupling in the following discussion.

Plus, the attitude model of Roll is regarded as the same as that of Pitch because of the symmetry of the Quad-Rotor structure. Thus, the attitude modeling is conducted aiming at the Roll angle only.

First, assume that the Quad-Rotor is a rigid body evolving in a three-dimensional space. In the body coordinate \mathcal{B} , the equations of motion for a vehicle of mass m subject to external force $\mathbf{F} \in \mathbb{R}$, torque $\boldsymbol{\tau} \in \mathbb{R}$ can be given as (Kendoul *et al.*, 2007, 2008)

$$m\dot{\mathbf{V}}^{\mathcal{B}} + \boldsymbol{\Omega} \times m\mathbf{V}^{\mathcal{B}} = \mathbf{F} \quad \mathbf{J}\dot{\boldsymbol{\Omega}} + \boldsymbol{\Omega} \times \mathbf{J}\boldsymbol{\Omega} = \boldsymbol{\tau} \quad (3.1)$$

where $\mathbf{V} = [u, v, w]$ and $\boldsymbol{\Omega} = [p, q, r]$ represent the linear and angular velocities in the body-fixed reference frame. The translational force \mathbf{F} is a combination of gravity, main thrust and lift forces from rotors.

Using Euler angles $\boldsymbol{\eta} = [\phi, \theta, \psi]$ and the convention ZYX , the rotation matrix from \mathcal{B} to the inertial reference frame \mathcal{I} is expressed as follows

$$\mathbf{R} = \begin{bmatrix} \cos \theta \cos \psi & \sin \phi \sin \theta \cos \psi - \cos \phi \sin \psi & \cos \phi \sin \theta \cos \psi + \sin \phi \sin \psi \\ \cos \theta \sin \psi & \sin \phi \sin \theta \sin \psi + \cos \phi \cos \psi & \cos \phi \sin \theta \sin \psi - \sin \phi \cos \psi \\ -\sin \theta & \sin \phi \cos \theta & \cos \phi \cos \theta \end{bmatrix} \quad (3.2)$$

Note that the matrix \mathbf{R} satisfies $\mathbf{R}^{-1} = \mathbf{R}^T$ and $\det(\mathbf{R}) = 1$. And considering the transformation between the two related coordinates as seen in Fig. 3, it is possible to separate the gravity from other forces and write the translational dynamics in \mathcal{I} as follows

$$\dot{\boldsymbol{\xi}} = \mathbf{v} \quad m\dot{\mathbf{v}} = \mathbf{R}\mathbf{F}^b - mg\mathbf{e}_3^i \quad (3.3)$$

with $\boldsymbol{\xi} = [x, y, z]$ and $\mathbf{v} = [\dot{x}, \dot{y}, \dot{z}]$ are the vehicle position and velocity in \mathcal{I} . In the above equation, g is the gravitational acceleration and \mathbf{F}^b is the resulting force (without gravity) acting on the airframe.

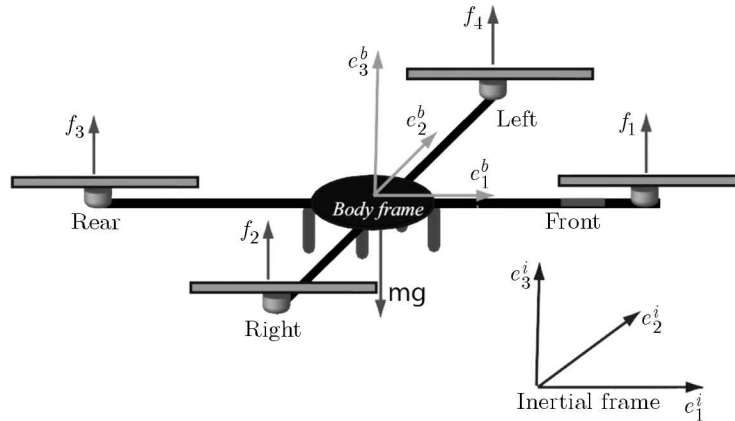


Fig. 3. Rigid body dynamics and the associated frames

Up to now, different techniques have been proposed to express the rotational dynamics such as the quaternion, rotation matrix \mathbf{R} or Euler angles. In the following, the Euler angles parametrization is employed to express the rotational dynamics in an appropriate form for control design.

To begin with, let us consider the kinematic relation between $\boldsymbol{\Omega}$ and $\dot{\boldsymbol{\eta}}$

$$\dot{\boldsymbol{\eta}} = \boldsymbol{\Phi}(\boldsymbol{\eta})\boldsymbol{\Omega} \quad (3.4)$$

with the Euler matrix

$$\boldsymbol{\Phi}(\boldsymbol{\eta}) = \begin{bmatrix} 1 & \sin \phi \tan \theta & \cos \phi \tan \theta \\ 0 & \cos \phi & -\sin \theta \\ 0 & \sin \phi \sec \theta & \cos \phi \sec \theta \end{bmatrix} \quad (3.5)$$

Note that the matrix Φ has singularities at $\theta = \pm\pi/2$, and its inverse matrix $\Psi(\eta) = \Phi^{-1}(\eta)$ is given

$$\Psi(\eta) = \begin{bmatrix} 1 & 0 & -\sin\theta \\ 0 & \cos\phi & \cos\theta\sin\phi \\ 0 & -\sin\phi & \cos\theta\sec\phi \end{bmatrix} \quad (3.6)$$

By differentiating Eq. (3.4) with respect to time, the second equation of Eq. (3.1) can be rewritten as

$$\ddot{\eta} = \dot{\Phi}\dot{\Omega} + \Phi\dot{\Omega} = \dot{\Phi}\Psi\dot{\eta} - \Phi\mathbf{J}^{-1}\mathbf{sk}(\Omega)\mathbf{J}\Omega + \Phi\mathbf{J}^{-1}\tau \quad (3.7)$$

The sk operation is defined here from \mathbf{R}^3 to $\mathbf{R}^{3\times 3}$ such that $\mathbf{sk}(x)$ is a skew symmetric matrix associated with the vector product $\mathbf{sk}(x)y := x \times y$.

As an assumption, the attitude angle is small enough to ignore the coupling, Φ and Ψ become identity matrices. Therefore, the differential equation of Roll motion can be obtained

$$\ddot{\phi} = f_{\phi}(\dot{\phi}, \phi) + J_{\phi}^{-1}\tau_{\phi} \quad (3.8)$$

with J_{ϕ} and τ_{ϕ} are the rotational inertia and torque around x axis, respectively, and $f_{\phi}(\dot{\phi}, \phi)$ represents a function about $\dot{\phi}$ and ϕ , which can be generated from Eq. (3.7).

Generally, the control input u to the actually obtained torque τ_{ϕ} can be thought as the first order delay system, which can be thought as a nonlinearity or disturbance to be absorbed to $f_{\phi}(\dot{\phi}, \phi)$. Then, we arrive at

$$\ddot{\phi} = f(\dot{\phi}, \phi) + J_{\phi}^{-1}u \quad (3.9)$$

In the differential equation above, the unknown parameter J_{ϕ} can be determined by experiments, while the detail information of $f(\dot{\phi}, \phi)$ still keeps unavailable. However, the control algorithm to be discussed does not involve the specific expression of f , so it is out of necessity to conduct a deep study about this function.

3.2. Memory based controller design

For attitude controller design, considering the nonlinearity and the strong coupling of real Quad-Rotor motion, it is of great importance to design the controller with good robustness in both stability and performance. Therefore, the memory based control technique is adopted to enhance the robustness (Song, 2006).

First, rewrite the differential equation

$$\ddot{\phi} = f(\dot{\phi}, \phi) + J_{\phi}^{-1}u \quad (3.10)$$

Defining the error $e = \phi - \phi^*$, the error system of the Roll model can be described as

$$\ddot{e} = f(\dot{\phi}, \phi) + J_{\phi}^{-1}u - \ddot{\phi}^* \quad (3.11)$$

where ϕ^* is the reference input angle.

For the convenience of processing, a new variable s is introduced

$$s = (q + k_0)e \quad \text{where} \quad k_0 > 0 \quad q = \frac{d}{dt} \quad (3.12)$$

The advantage of this treatment is that the original 2-order tracking problem in respect of ϕ is reduced to 1-order stabilization in s . Even if the system equation grows to n -order, this processing approach can also be applied by just adjusting s to be $s = (q + k_0)^{n-1}e$.

In order to substitute \ddot{e} , we only need to differentiate s once for the input, leading to

$$\dot{s} = (q + k_0)\dot{e} = \ddot{e} + k_0\dot{e} \tag{3.13}$$

Replacing \ddot{e} above by Eq. (3.11), we get

$$\dot{s} = f(\dot{\phi}, \phi) - \ddot{\phi}^* + k_0\dot{e} + J_\phi^{-1}u \tag{3.14}$$

Now, define the control input as

$$J_\phi^{-1}u = v + \eta(\cdot) \tag{3.15}$$

where $\eta(\cdot) = \ddot{\phi}^* - k_0\dot{e}$, and v is a memory-based compensator accounting for system nonlinearities and other disturbances. The closed-loop system in terms of s becomes

$$\dot{s} = f(\ddot{\phi}, \phi) + v \tag{3.16}$$

By Euler differentiation, we get

$$s_{k+1} = s_k + (f_k + v_k)T \tag{3.17}$$

Here, T is the sampling period. Now performing backward time-shift in the above equation, we have

$$s_k = s_{k-1} + (f_{k-1} + v_{k-1})T \tag{3.18}$$

Subtracting Eq. (3.18) from Eq. (3.17), gives

$$s_{k+1} = 2s_k - s_{k-1} + (f_k + v_k)T - (f_{k-1} + v_{k-1})T \tag{3.19}$$

Now define v_k as

$$v_k = w_0v_{k-1} + w_1s_k + w_2s_{k-1} \tag{3.20}$$

with $w_0 = 1, w_1 = -2/T, w_2 = 1/T$. Then, Eq. (3.19) can be rewritten as

$$s_{k+1} = (f_k - f_{k-1})T = T\Delta f_k \tag{3.21}$$

For a fairly small T , $\Delta f_k \approx T(df/dt) | t = kT$, so we have

$$|s_{k+1}| \leq T^2\lambda \tag{3.22}$$

λ in the above equation is defined as

$$\lambda = \max\left(\left|\frac{df}{dt}\right| \Big| t = 0, T, 2T, \dots, nT\right) \tag{3.23}$$

Considering the definition of s which can be regarded as a sliding hyperplane with a chattering range of $T^2\lambda$, when s is convergent, the tracking error e and its derivative \dot{e} are also convergent.

The equations above indicate that if the variation of function f is not infinitely fast, the tracking error and its derivative would be considerable small (since T is very small in general).

To summarize, for the above attitude model with a sampling period of T and reference input ϕ^* , the memory based controller is designed as (by subtracting $u_{k-1} = J_\psi(v_{k-1} + \eta_{k-1})$ from Eq. (3.15))

$$u_k = u_{k-1} - \frac{2J_\phi}{T}(\dot{e}_k + k_0e_k) + \frac{J_\phi}{T}(\dot{e}_{k-1} + k_0e_{k-1}) + J_\phi(\eta_k - \eta_{k-1}) \tag{3.24}$$

with J_ϕ being the rotational torque, $\eta(\cdot) = \ddot{\phi}^* - k_0\dot{e}$.

For simplification, $\eta(\cdot)$ can be merged into $f(\cdot)$, so the control input expression is driven to

$$u_k = u_{k-1} - \frac{2J_\phi}{T}(\dot{e}_k + k_0 e_k) + \frac{J_\phi}{T}(\dot{e}_{k-1} + k_0 e_{k-1}) \quad (3.25)$$

To verify the effectiveness of the controller, we carried out a series of simulations. For the attitude system of Eq. (3.10), the detailed information of function $f(\cdot)$ keeps unknown, so it is quite necessary to change $f(\cdot)$ in different forms

$$f_1(\dot{\phi}, \phi) = \dot{\phi} + \phi + 1 \quad f_2(\dot{\phi}, \phi) = \dot{\phi}\phi + \dot{\phi} + \phi + 1 \quad (3.26)$$

The simulation results of the controller are shown in Fig. 4. We can see that for different form of function $f(\cdot)$ the memory based controller can keep excellent tracking performance, so that the good robustness is realized.

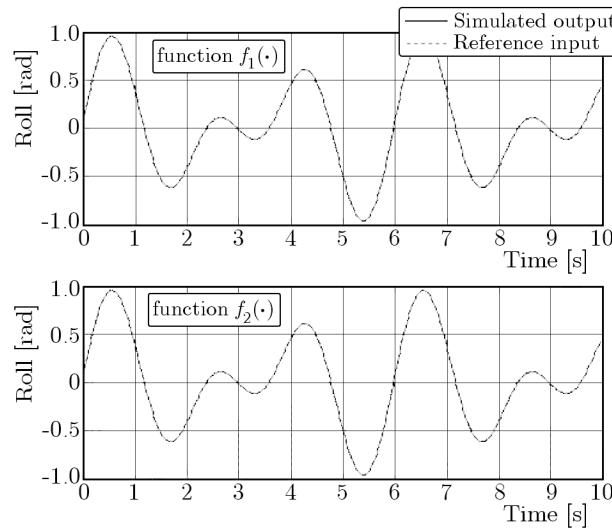


Fig. 4. Simulation results of memory based controller ($T = 0.02\text{s}$, $K_0 = 1$, $J = 0.173$)

4. Altitude modeling and controller design

The altitude results from the combination force of four rotors, so the model can be easily obtained. Then the LQG controller based on optimal controller is designed.

4.1. Altitude modeling

The altitude of the vehicle is controlled by the rotational speed of four rotors. According to the previous work on the rotor performance test, the relationship between the control input u and generated thrust F can be supposed as one order system

$$F(s) = \frac{k}{1 + T_1 s} u(s) \quad (4.1)$$

Here k and T_1 are the constant parameters of the one order system. The relations between thrust F and position can be represented as

$$\ddot{Z} = a = \frac{FC_\phi C_\theta - f_Z - mg}{m} \quad (4.2)$$

where Z is the altitude, a is the acceleration of z axis, $C_x = \cos x$, ϕ , θ are Roll and Pitch angles, respectively, f_Z is the air-resistance, m is the mass of the plant and g is the gravitational acceleration. In general, the Quad-Rotor MAV mainly moves at a low speed, and the lean angle is about 20 degree. Ignoring the air-resistance, the linearization of Eq. (4.2) can be given

$$\ddot{Z} = a = \frac{F - mg}{m} \quad (4.3)$$

From Eq. (4.1) and Eq. (4.3), we can get the transfer function from control input to position as follows

$$G(s) = \frac{Z(s)}{u(s)} = \frac{k}{(1 + T_1 s)ms^2} \quad (4.4)$$

To determine the unknown parameters, an information set of input and output data from the real flight is applied to the system identification tool. In order to verify the accuracy of the identified model, we analyze the system time historical response, and the result is shown in Fig. 5. The axis y represents the altitude of the MAV by setting the start point as zero.

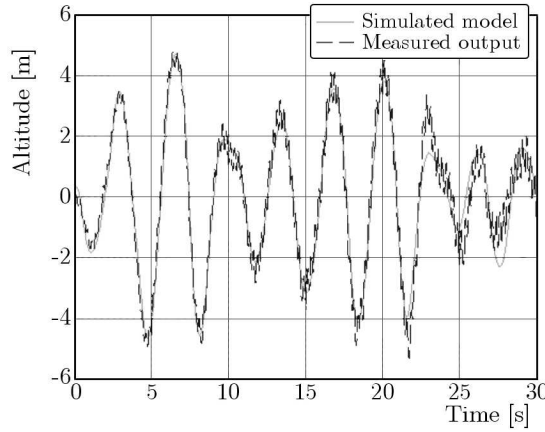


Fig. 5. Cross validation result of the altitude model

4.2. Optimal controller design

The altitude model is insensitive to the outer interference. To reduce the control difficulty, the LQI control method (Wang *et al.*, 2008) is applied. LQI is a preferable design method of servo controllers based on the optimal control theory.

Rewrite transfer function Eq. (4.4) to the state-space equation

$$\dot{\mathbf{x}}(t) = \mathbf{A}\mathbf{x} + \mathbf{B}\mathbf{u} \quad \mathbf{y} = \mathbf{C}\mathbf{x} \quad (4.5)$$

To enhance the controller performance in tracing, a new state variable $\mathbf{x}_r(t)$ is constructed as the integral value of the displacement error: $\mathbf{x}_r(t) = \int [\mathbf{y}(t) - \mathbf{r}(t)] dt$, and the following expansion system is established

$$\dot{\mathbf{x}}_a(t) = \begin{bmatrix} \dot{\mathbf{x}}(t) \\ \dot{\mathbf{x}}_r(t) \end{bmatrix} = \begin{bmatrix} \mathbf{A} & \mathbf{0} \\ -\mathbf{C} & \mathbf{0} \end{bmatrix} \begin{bmatrix} \mathbf{x}(t) \\ \mathbf{x}_r(t) \end{bmatrix} + \begin{bmatrix} \mathbf{B} \\ \mathbf{0} \end{bmatrix} \mathbf{u}(t) + \begin{bmatrix} \mathbf{0} \\ \mathbf{I} \end{bmatrix} \mathbf{r}(t) = \mathbf{A}^* \mathbf{x}_a(t) + \mathbf{B}^* \mathbf{u}(t) + \begin{bmatrix} \mathbf{0} \\ \mathbf{I} \end{bmatrix} \mathbf{r}(t) \quad (4.6)$$

where $\mathbf{x}_a(t)$ is the state variable of the expanded system, $\mathbf{r}(t)$ is the reference input, \mathbf{I} is a identify matrix and

$$\mathbf{A}^* = \begin{bmatrix} \mathbf{A} & \mathbf{0} \\ -\mathbf{C} & \mathbf{0} \end{bmatrix} \quad \mathbf{B}^* = \begin{bmatrix} \mathbf{B} \\ \mathbf{0} \end{bmatrix} \quad (4.7)$$

The LQI control corresponds to the optimal control problem for the system above in terms of the quadratic form criterion function

$$\mathbf{J} = \frac{1}{2} \int_0^{\infty} [\mathbf{x}_a^T \mathbf{Q} \mathbf{x}_a(t) + \mathbf{u}^T(t) \mathbf{R} \mathbf{u}(t)] dt \quad (4.8)$$

The optimal control is to determine the control input $\mathbf{u}(t)$ to minimize the function. In view of Eq. (4.8), we have the Hamiltonian

$$\mathbf{H} = \frac{1}{2} \mathbf{x}_a^T(t) \mathbf{Q} \mathbf{x}_a(t) + \frac{1}{2} \mathbf{u}^T(t) \mathbf{R} \mathbf{u}(t) + \boldsymbol{\lambda}^T(t) [\mathbf{A}^*(t) \mathbf{x}_a(t) + \mathbf{B}^*(t) \mathbf{u}(t)] \quad (4.9)$$

Then, the adjoint equation and boundary condition can be obtained

$$\begin{aligned} \dot{\boldsymbol{\lambda}}(t) &= -\frac{\partial \mathbf{H}}{\partial \mathbf{x}_a} = -\mathbf{A}^{*\top}(t) \boldsymbol{\lambda}(t) - \mathbf{Q} \mathbf{x}_a(t) & \boldsymbol{\lambda}(T) &= \mathbf{S} \mathbf{x}_a(T) \\ \frac{\partial \mathbf{H}}{\partial \mathbf{u}} &= \mathbf{R} \mathbf{u}(t) + \mathbf{B}^{*\top}(t) \boldsymbol{\lambda}(t) = \mathbf{0} \end{aligned} \quad (4.10)$$

with the condition that \mathbf{R} is positive, the control input is obtained

$$\mathbf{u}(t) = -\mathbf{R}^{-1} \mathbf{B}^{*\top}(t) \boldsymbol{\lambda}(t) \quad (4.11)$$

Assume that the relationship between $\boldsymbol{\lambda}(t)$ and state variables $\mathbf{x}_a(t)$ can be expressed as

$$\boldsymbol{\lambda}(t) = \mathbf{P} \mathbf{x}_a(t) \quad (4.12)$$

in which the matrix \mathbf{P} can be obtained from the Riccati equation

$$\mathbf{P} \mathbf{A}^* + \mathbf{A}^{*\top} \mathbf{P} - \mathbf{P} \mathbf{B}^* \mathbf{R}^{-1} \mathbf{B}^{*\top} \mathbf{P} + \mathbf{Q} = \mathbf{0} \quad (4.13)$$

Replacing the $\boldsymbol{\lambda}(t)$ in Eq. (4.11) by Eq. (4.12), the feedback gain \mathbf{F} can be given as follows and the control input is obtained accordingly

$$\begin{aligned} \mathbf{F} &= [F_1, F_2] = \mathbf{R}^{-1} \mathbf{B}^{*\top} \mathbf{P} \\ \mathbf{u}(t) &= -F_1 \mathbf{x}(t) - F_2 \mathbf{x}_r(t) = -F_1 \mathbf{x}(t) - F_2 \int_0^t \mathbf{e}(t) dt \end{aligned} \quad (4.14)$$

Since the controller is based on the state feedback, it is necessary to observe all the state conditions. In the altitude model obtained above, there are three state variables. Although the acceleration and the altitude can be measured by the onboard sensors, there is still one state variable that cannot be observed. Therefore, a Kalman filter is chosen to estimate the unknown state variable and it can also filter the noise meanwhile, so that the control quality is improved.

5. Experiments and experiments results

In order to verify the performance of our platform and the technique of attitude and altitude controller design, real actual flight experiments are carried out. The reference is given to the MAV by the operator using 72 MHz PPM Propo. The flight data are gathered via XBee-pros which conduct the communication between the aircraft and the ground station.

5.1. Attitude experiments

The effectiveness of the attitude controller is confirmed by keeping the MAV hovering or moving at a high speed. So the attitude control experiment is divided into two parts: hovering and tracking experiments.

Results from a hovering test are shown in Fig. 6. We can see from the figure that, when the reference is set to zero, the airframe can almost keep hovering with deviation of ± 3 degrees. Considering the influences of wind and other interference, the result is acceptable.

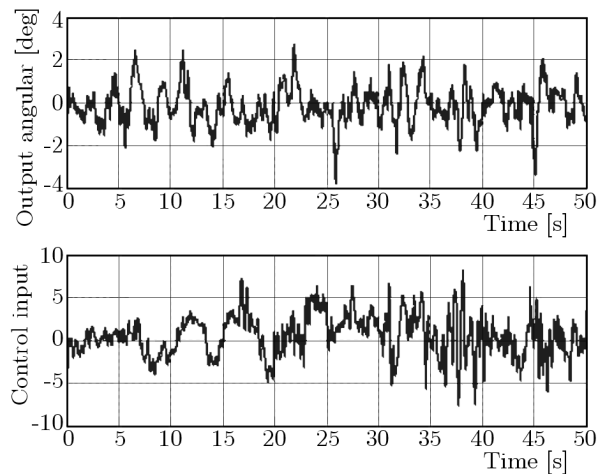


Fig. 6. Hovering experimental result

The tracking performance of the controller is shown in Fig. 7. It is clear that the output angle successfully tracks the reference at both low and high frequencies, indicating that fairly good tracking results are maintained.

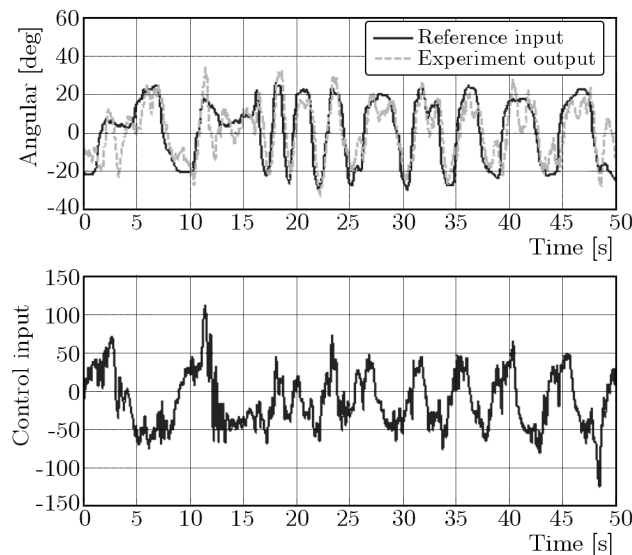


Fig. 7. Attitude experimental result

As to the system robustness which is one of the most interesting features of memory controller, a comparison is conducted between the LQG and memory based control technique for attitude control with a 300 g payload. But once the LQG controller is installed, the flight performance degrades badly, making the operation of the vehicle difficult. Therefore, only the experimental result for the robustness of memory controller is shown here. Figure 8 indicates

that the controller is almost completely insensitive to model changes and the good robustness is obtained.

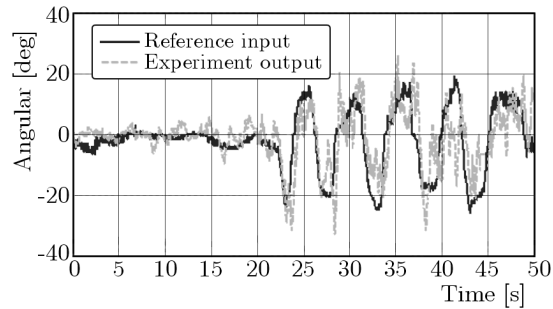


Fig. 8. Robust experimental result

5.2. Altitude experiments

To verify the stability and tracking performance of the designed altitude controller, a step signal of 5 m is given to the Quad-Rotor after hovering stably for some time in a fixed altitude. Results from the flight test are shown in Fig. 9. The real time experimental result follows the simulation result well and the output successfully tracks the reference input in about 5 s with a 0.5 m overshoot. The controller has also a good stability with the stable control input.

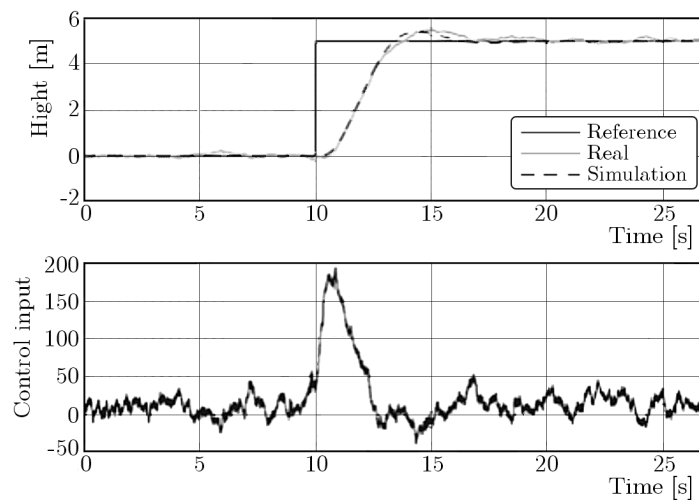


Fig. 9. Altitude experimental result

6. Conclusion

In this research, a brief introduction is given to the Quad-Rotor which is selected as our controlled object, and then the techniques of attitude and altitude controller design are discussed. For the attitude, memory based controller is proposed due to its insensitivity to the model errors, parametric uncertainties and other disturbances. Whereas in the altitude control, a model based optimal controller is designed. The desired features of the control algorithm are all well proven in real-time flight experiments. What is more, by developing the memory controller, the attitude controller also obtains excellent robustness.

Our future work will focus on indoor obstacle avoidance which is in high demand of the flight stability. Therefore, on the present basis of the attitude control technique, a relatively good performance will be achieved.

Acknowledgement

This work was supported by National Outstanding Youth Science Foundation (No. 61125306), National Natural Science Foundation of Major Research Plan (No. 91016004), The National Natural Science Foundation of China (Grant No. 61004046).

References

1. ACHELNIK M., BACHRACH A., HE R., PRENTICE S., ROY N., 2009, Stereo vision and laser odometry for autonomous helicopters in gps-denied indoor environments, *Proceedings of the SPIE Conference on Unmanned Systems Technology XI*, Orlando, FL
2. Ascending Technologies GmbH, <http://www.asctec.de>.
3. BACHRACH A., HE R., ROY N., 2009, Autonomous flight in unstructured and unknown indoor environments, *Proceedings of EMMAV*
4. HOFFMANN G.M., HUANG H., WASLANDER S.L., TOMLIN C.J., 2011, Precision flight control for a multi-vehicle quadrotor helicopter testbed, *Control Engineering Practice*, **19**, 9, 1023-1036
5. <http://www.draganfly.com/>
6. KENDOUL F., 2012, Survey of advances in guidance, navigation, and control of unmanned rotorcraft systems, *Journal of Field Robotics*, **29**, 2, 315-378
7. KENDOUL F., FANTONI I., LOZANO R., 2008, Asymptotic stability of hierarchical inner-outer loop-based flight controllers, *Proceedings of the 17th IFAC World Congress*, Seoul, Korea, 1741-1746
8. KENDOUL F., LARA D., FANTONI I., LOZANO R., 2007, Real-time nonlinear embedded control for an autonomous Quad-Rotor helicopter, *AIAA Journal of Guidance, Control, and Dynamics*, **30**, 4, 1049-1061
9. MARTINEZ V.M., 2007, Modeling of the flight dynamics of a quadrotor helicopter, A MSc Thesis in Cranfield University
10. NONAMI K., KENDOUL F., SUZUKI S., WANG W., NAKAZAWA D., 2010, *Autonomous Flying Robots-Unmanned Aerial Vehicles and Micro Aerial Vehicles*, Springer
11. RUDIN K., HUA M.D., DUCARD G., 2011, A robust controller and its application to quadrotor helicopters, *Proceedings of the 18th IFAC World Congress*, Italy
12. SONG Y.D., 2006, Memory-based control of nonlinear dynamic systems. Part I – Design and analysis, *Industrial Electronics and Applications, 2006 1ST IEEE Conference on*
13. TAYEBI A., MCGILCARY S., 2006, Attitude stabilization of a VTOL quadrotor aircraft, *IEEE Transactions on Control Systems Technology*, **14**, 3, 562-571
14. WANG W., NONAMI K., HIRATA M., 2008, Model reference sliding mode control of small helicopter X.R.B based on vision, *International Journal of Advanced Robotic Systems*, **5**, 3, 235-242
15. WANG W., SONG Y.Z., NONAMI K., CHENG Y., ZHOU Y., WANG F., 2011, Attitude controller design for a six-rotor type MAV, *Key Engineering Materials*, **480-481**, 1155-1160
16. XIA M., ZHANG Y., WENG L., YE X., 2012, Fashion retailing forecasting based on extreme learning machine with adaptive metrics of inputs, *Knowledge-Based Systems*, **36**, 253-259